TISSUE ENGINEERING: Part B
Volume 17, Number 5, 2011

DOI: 10.1089/ten.teb.2011.0230

Potential for Imaging Engineered Tissues with X-Ray Phase Contrast

Alyssa Appel, M.S.,[1,2] Mark A. Anastasio, Ph.D.,[3] and Eric M. Brey, Ph.D.[1,2]

As the field of tissue engineering advances, it is crucial to develop imaging methods capable of providing detailed three-dimensional information on tissue structure. X-ray imaging techniques based on phase-contrast (PC) have great potential for a number of biomedical applications due to their ability to provide information about soft tissue structure without exogenous contrast agents. X-ray PC techniques retain the excellent spatial resolution, tissue penetration, and calcified tissue contrast of conventional X-ray techniques while providing drastically improved imaging of soft tissue and biomaterials. This suggests that X-ray PC techniques are very promising for evaluation of engineered tissues. In this review, four different implementations of X-ray PC imaging are described and applications to tissues of relevance to tissue engineering reviewed. In addition, recent applications of X-ray PC to the evaluation of biomaterial scaffolds and engineered tissues are presented and areas for further development and application of these techniques are discussed. Imaging techniques based on X-ray PC have significant potential for improving our ability to image and characterize engineered tissues, and their continued development and optimization could have significant impact on the field of tissue engineering.

Introduction

In the United States alone, ~50,000 patients are added to the organ transplant list annually. However, due to a severe shortage in donor organs only around 28,000 of these patients receive an organ each year.[1] In addition to the need for whole organ transplants, donor tissue is required for many of the over 5.2 million reconstruction procedures performed annually in the United States.[2] Tissue engineering and regenerative medicine have emerged as fields that could provide alternatives to traditional methods of tissue reconstruction and organ replacement. These methods could reduce dependence on donor organs, the need for autologous tissue or prostheses for reconstruction, and complications associated with these procedures (immune rejection, donor-site morbidity, etc.).

A primary limitation to the study of engineered tissues is the inability to quantitatively analyze the three-dimensional (3D) structure of the tissue formed. Quantitative 3D imaging tools are needed that enable a more thorough analysis of tissue formation to better understand biological response following a tissue engineering strategy. A number of techniques are available for imaging engineered tissues (Table 1). Optical methods (e.g., confocal microscopy and optical coherence tomography) have received significant attention, but their relatively limited tissue penetration leads to imaging of only superficial structures. In addition, these methods often require addition of exogenous agents to label features within the engineered tissues. Ultrasonography and photoacoustic imaging methods have also been employed[3] but cannot simultaneously achieve high spatial resolution, deep tissue penetration, and good tissue contrast. Magnetic resonance imaging (MRI) has good soft tissue contrast in the absence of exogenous agents. However, MRI can yield poor spatial resolution when imaging the large tissue volumes required for many tissue engineering applications and cannot be used to image bone or biomaterials that lack water in the absence of exogenous contrast agents.

Traditional (absorption-based) X-ray imaging technologies can possess excellent spatial resolution with deep tissue penetration and provide significant quantitative data about calcified tissue structure. There have been many studies where microcomputed tomography (μCT) was used to analyze the 3D structure of engineered tissues and a number of excellent reviews are available on this topic.[4,5] Improvements in the spatial resolution has allowed X-ray techniques to provide important insight into engineered tissues, but the reliance of X-ray and μCT/CT techniques on absorption

[1]Department of Biomedical Engineering and Pritzker Institute of Biomedical Science and Engineering, Illinois Institute of Technology, Chicago, Illinois.
[2]Research Service, Hines Veterans Administration Hospital, Hines, Illinois.
[3]Department of Biomedical Engineering, Washington University in St. Louis, St. Louis, Missouri.

Table 1. Common Three-Dimensional Imaging Techniques Available for Analysis of Engineered Tissues

3D imaging technique	*Spatial resolution*	*Imaging depth*	*Soft tissue contrast*	*Calcified tissue contrast*
Confocal microscopy	Excellent	Poor	Good	Poor
Optical coherence tomography (OCT)	Good	Poor	Good	Poor
Magnetic resonance imaging (MRI)	Poor	Excellent	Excellent	Poor
Ultrasound	Good	Excellent	Poor	Good
Photoacoustic imaging	Good	Good	Excellent	Poor
Absorption-based X-ray CT	Excellent	Excellent	Poor	Excellent

3D, three-dimensional; CT, computed tomography.

contrast alone limits their broad application. Absorption contrast results in little or no information on materials with low atomic numbered elements, including soft tissues, cells, vasculature, and many biomaterials. Some polymer scaffolds generate contrast in μCT, but the contrast is poor when the scaffolds are used in bioreactor conditions or embedded in tissues. In addition, materials with high water content (hydrogels) investigated in a number of tissue engineering applications generate no X-ray absorption contrast. Heavy metal contrast agents can be used to enhance absorption of specific tissue features, such as microvascular structure[6,7] and cartilage[8] in engineered tissues.[9,10] However, reliance on exogenous agents limits the number of features that can be observed in a given sample, and these agents often exhibit poor tissue and cell compatibility.

In the past decade, novel X-ray imaging techniques based on phase contrast (PC) have shown promise for biomedical application due to their ability to provide information about soft tissue structure without the use of exogenous contrast agents. The principal advantage is that X-ray PC imaging methods are sensitive to alternative physical properties of tissues, and can differentiate between tissues that have very similar or even identical X-ray absorption properties. In some cases, X-ray PC techniques can simultaneously provide information on soft tissue, biomaterial, and calcified tissue structure all in the absence of contrast agents. The ability of X-ray PC contrast techniques to retain the excellent spatial resolution, tissue penetration, and calcified tissue contrast of absorption-based techniques (Table 1), with drastically improved soft tissue and biomaterial contrast, suggests that they have great potential for evaluation of engineered tissues.

The goal of this review article is to describe the extensive potential of X-ray PC techniques as tools for analyzing engineered tissues. We will review the physical principles of X-ray PC imaging and four distinct implementations of the method. Subsequently, we will discuss their potential for imaging tissue features of significance to many tissue engineering applications and examine recent reports of application of X-ray PC to engineered tissues and biomaterial scaffolds. Finally, we will identify areas where the continued development and optimization of X-ray PC imaging is needed and could have significant impact on the field of tissue engineering.

Basic Principles of PC X-Ray Imaging

A number of X-ray PC imaging methods that have dramatic advantages over conventional radiographic X-ray imaging systems are being actively developed.[11–14] The advantages of PC imaging stem from the fact that, at diagnostic X-ray energies, the refractive-index variations of tissue are generally orders of magnitude greater than variations in the X-ray attenuation coefficient.[11] This is because refraction contrast decreases as the X-ray energy squared, whereas absorption contrast drops as the energy to the fourth power. Therefore, PC imaging offers the potential for very-low-dose imaging[15] by using X-ray energies that are traditionally considered too high to be useful for imaging soft tissue. The ability to detect low-contrast tissue features, while simultaneously reducing the radiation dose, underlies the great potential of X-ray PC imaging for biomedical imaging applications.[16]

As opposed to conventional radiographic methods, X-ray PC imaging requires the irradiating X-ray beam to possess a sufficient degree of coherence so that wave-like phenomenon such as refraction and interference can be observed. To understand the basic image formation principles of PC imaging, consider an idealized scenario in which a monochromatic X-ray plane-wave $U_i(x, y, z)$, propagating along the z-axis, irradiates an object. The transmitted wavefield $U_t(x, y;z=0)$ on the contact plane behind the object is given by[17]

$$U_t(x,y;z=0) = U_i(x,y,z)\exp\left[j\phi(x,y) - \frac{\mu(x,y)}{2}\right] \equiv A(x,y)\exp\left[j\phi(x,y)\right],$$

where

$$\phi(x,y) = -\frac{2\pi}{\lambda}\int dz\ \delta(\vec{r}) \text{ and } \mu(x,y) = \frac{4\pi}{\lambda}\int dz\ \beta(\vec{r}),$$

λ is the wavelength, and $\delta(\vec{r})$ and $\beta(\vec{r})$ denote the real and imaginary components of the X-ray refractive index. The quantities $\phi(x, y)$ and $\mu(x, y)$ represent the projected phase and linear attenuation coefficient that characterize the object, respectively. Note that if the intensity $I(x, y;0) = |U_t(x, y;0)|^2$ on the contact plane were recorded, the resulting image would correspond to a conventional absorption-based radiography that is determined solely by the X-ray absorption properties.

An imaging system allows PC effects to be observed only when the transmitted X-ray wavefield $U_t(x, y;0)$ is modified in some way before recording the intensity of the modified wavefield. In this way, variations in $\phi(x, y)$ introduced by the object can result in variations in the recorded intensity. Four implementations of PC imaging that achieve this are described below. The variations in the recorded image that are due to variations in $\phi(x, y)$ are referred to as PC effects. In general, the raw measured image will have a mixed contrast that arises from both PC and conventional absorption

contrast. In some implementations, multiple images are acquired that correspond to different configurations of the imaging system, and then computational methods can be utilized to un-mix the contrast mechanisms and obtain separate images that contain only PC or absorption contrast. Additionally, for some implementations, a third dark-field image can be computed that contains information regarding the ultra-small-angle-scattering properties of the object.

Implementations of X-Ray PC Imaging

In this section, we review four implementations of X-ray PC imaging that are maturing rapidly and likely to have a widespread impact on the field of tissue engineering in the near future. The operating principles of each technique and its relative advantages and disadvantages are described. The reader who is interested in a more extensive review of X-ray PC techniques with substantial technical details is encouraged to examine a number of other excellent reviews.[11,18–20]

Propagation-based PC imaging

The first, and simplest technique to implement, is known as in-line holography or propagation-based PC. This setup is similar to conventional absorption-based X-ray imaging; however, the detector is placed at a distance further than what is used for attenuation based (Fig. 1A). In typical absorption-based X-ray systems, the detector is placed directly behind, or relatively close to, the object. In propagation-based PC imaging, the transmitted X-ray wavefield is allowed to propagate behind the object before its intensity is recorded by a detector placed downstream. The act of free space wavefield propagation induces PC effects into the measured intensity image. This results in an edge enhancement effect at image locations corresponding to the projected tissue interfaces. The object-to-detector distance can be chosen to optimize this edge enhancement while minimizing image blurring due to partial spatial coherence of the X-ray wavefield. Many variations of the technique have been developed by taking images at different detector distances, allowing production of either two separate images representing phase and absorption contrast[21] or a single image representing varying degrees of combination of phase and absorption effects.[22,23] This method can be implemented with a polychromatic beam from a microfocus X-ray tube without using X-ray optical elements, making it one of the simplest to implement in laboratory and clinical settings.

X-ray interferometry

The second PC technique is based on Triple Laue interferometry. This setup involves three crystals (Fig. 1B). The first, called the splitter crystal, divides a coherent beam into two identical beams that diverge through Laue diffraction. The second crystal causes the beams to converge toward one another. The object to be imaged is placed in the path of one of the converging beams. The two beams interfere at the third crystal and the phase changes created by the object are measurable as intensity variations in the interference patterns. This system is able to detect phase shifts of the beam due to the object by comparing the two converging beams. Both phase and absorption images can be constructed from this image.[24,25] This form of interferometry is the most sensitive method for PC; however, it is limited to a small field of view. In addition, the system requires a coherent beam available only with a synchrotron source and high system stability. A synchrotron is a large particle accelerator available in only a limited number of locations worldwide and not able to fit in a laboratory. Therefore, this PC imaging scheme cannot be performed with a standard X-ray source.

Differential PC imaging using X-ray gratings

The third technique is known as Differential PC imaging based on the Talbot effect.[18,26–28] This method utilizes two or three X-ray gratings depending on the X-ray source (Fig. 1C).

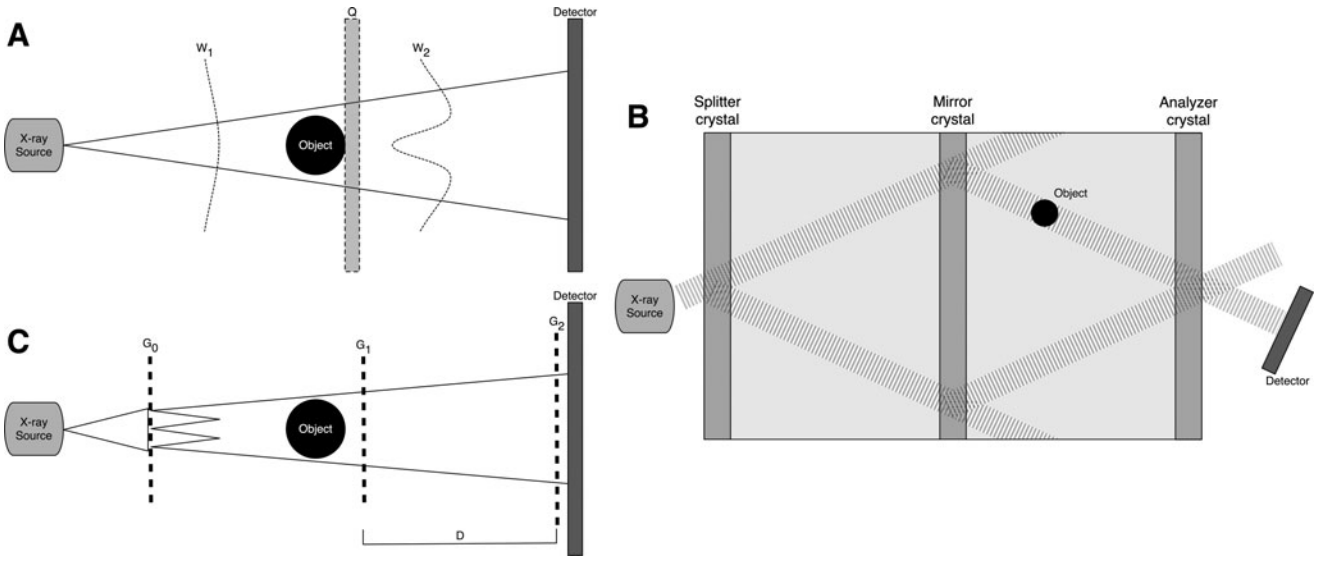

FIG. 1. Schematics of X-ray PC implementations. **(A)** Propagation-based imaging: W_1 and W_2 represent the wavefield before and after interaction with the object, and Q is the position of the detector in traditional absorption-based X-ray imaging. **(B)** X-ray interferometry. **(C)** Differential phase-contrast imaging. D represents the fractional Talbot distance. PC, phase contrast.

Two of the gratings, the phase (G1) and analyzer absorption (G2) gratings, are placed between the object and detector and image contrast is formed through the combined effect of the two gratings. The G1 grating imprints periodic phase modulations onto the incoming wavefield by acting as a phase mask. Through the Talbot effect, the phase modulation is transformed into an intensity modulation by placing G2 at distances defined as fractional Talbot distances. The intensity modulation forms a linear periodic fringe pattern perpendicular to the optical axis and parallel to the lines of G1. The G2 grating, with absorbing lines and the same periodicity and orientation as the fringes created by G1, is placed in the detection plane, immediately in front of the detector.[18] The G1 grating is moved in relation to the G2 grating and a detected intensity curve is created in relation to their relative positions. When the object is present, the change in the measured intensity curve is detected and the X-ray absorption, refraction, and ultra-small-angle X-ray scatter (USAXS) properties of the object can be calculated.[18,28–31] The Differential PC imaging technique is advantageous because it can image a large field of view and can tolerate a certain degree of beam polychromaticity and can therefore be implemented with X-ray tube sources. In that case, a source grating (G0) can be employed to create an array of independent line sources that can be used to form a Talbot-Lau Interferometer.[28]

Analyzer-based imaging using crystals

The final category of X-ray PC imaging we consider is analyzer-based imaging. In analyzer methods, an X-ray beam is prepared by use of a crystal monochromator, which results in a collimated and monochromated incident wavefield. This wavefield irradiates an object and is subsequently diffracted by an analyzer crystal. Based on properties of the analyzer crystal, X-rays travelling at or near the crystal's Bragg angle are selected and ultimately passed on to the intensity detector. Two different types of analyzer crystals can be used leading to two different imaging techniques. The first category uses a Bragg's Analyzer crystal which reflects X-rays (Fig. 2A). In this case, the analyzer crystal is rotated to different angles (on a microradian scale) and only the X-rays that satisfy Bragg's condition will reflect and be detected. Measurements are taken at several different angles of the analyzer crystal to generate an angular intensity curve known as a rocking curve. When an object is present in the pathway, changes in this rocking curve can be detected and used to reconstruct images that represent the absorption, refraction, and USAXS properties of the object.

Several imaging techniques have been developed to reconstruct the object properties from the measurements described above. Diffraction enhanced imaging (DEI) uses intensity measurements at analyzer angles at the full width half maximum on either side of the rocking curve. Two separate absorption and refraction contrast images can be mathematically calculated from these data.[32,33] However, this technique does not account for USAXS[34] effects, which can result in inaccuracies in the images. In scatter-based DEI, measurements are collected at the peak and toe ($\sim$15% of the max) of the rocking curve and this information is used to calculate X-ray absorption and USAXS images.[35] This method assumes that the probing X-ray wavefield experiences no net refraction due to large-scale variations in the refractive index distribution, which is typically not a valid assumption for medical imaging.[34] Extended DEI (eDEI) requires three data points taken at the peak and at the two maxima of the second derivative of the rocking curve.[36] This method results in separate images representing the absorption, refraction, and USAXS properties of the object.[34,36]

While the eDEI reconstruction method produces three images, the images can sometimes contain crosstalk and therefore represent a mixture of object properties. Multiple image radiography (MIR) can be implemented to reduce this crosstalk between object property images. MIR produces absorption, refraction, and USAXS-based images by taking data at multiple points, usually more than five, on the rocking curve. The absorption image is similar to a conventional radiograph; however, it is free of the undesired scatter that is usually present and reduces image contrast. The refraction image depicts the effect of small beam deflections due to slowly varying refractive index variations in the object and is determined from the shift in the rocking curve distribution when the object is present. The USAXS quantifies angular divergence of the beam caused by the presence of multiple beam refraction from sub-pixel-sized scatters and represents broadening of the rocking curve.[13,37]

Other analyzer-based systems employ a Laue-case dynamic diffraction crystal as an analyzer to form a technique known as X-ray Dark Field Imaging. In this case, the X-ray beam components that satisfy Bragg's condition are transmitted straight through the analyzer crystal toward one detector. All other X-rays not satisfying the condition pass through and are diffracted to another detector (Fig. 2B). This allows for PC and absorption images to be produced simultaneously without any need for reconstruction.[38–40]

All four PC imaging techniques provide images with good contrast and information not available with traditional

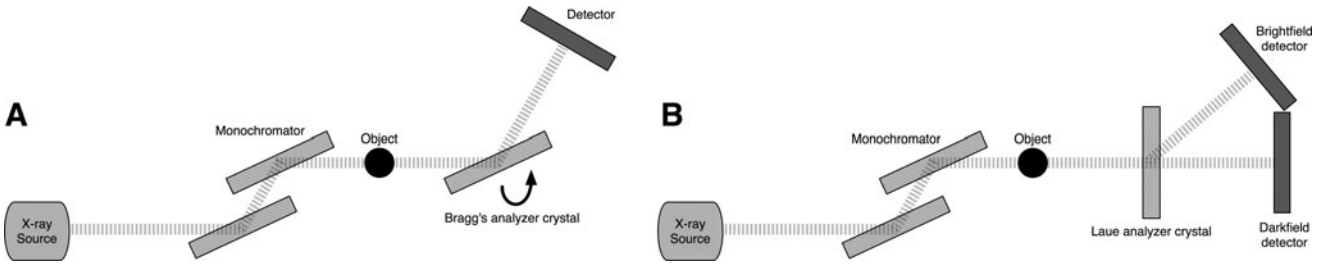

FIG. 2. Schematics of analyzer-based X-ray PC implementations. **(A)** Diffraction-enhanced imaging and multiple image radiography (MIR) and **(B)** X-ray dark-field imaging.

attenuation-based X-ray imaging. However, sensitivity varies between methods and an increase in sensitivity is often balanced by a greater complexity for implementing the system. For example, analyzer-based systems have the highest potential sensitivity but are more difficult to implement. Interferometric systems are the most sensitive, followed by analyzer-based, grating based, and propagation-based imaging. While propagation-based imaging is the easiest to implement followed by grating based, analyzer based, and intereferometric imaging. In addition, a researcher must also consider the importance of signal resulting from USAXS. If a given material or tissue is expected to generate contrast via X-ray scatter, then grating or analyzer-based imaging systems should be used.

Applications of X-Ray PC Imaging

These implementations of X-ray PC imaging have been evaluated for imaging a number of tissues and biomaterials that produce little contrast when imaged with traditional absorption-based techniques or other modalities. Two areas where X-ray PC has proven to be particularly advantageous are in imaging orthopedic tissues and vasculature, applications with relevance to a number of engineered tissues. In addition, PC techniques have recently been used to image cells and biomaterials addressing problems consistent with those encountered in tissue engineering. These studies are described in more detail in the following sections.

Orthopedic tissues

Conventional absorption-based X-ray imaging is commonly used to examine bone structure and to identify injury to ligaments and tendons. X-ray PC imaging has demonstrated several advantages over traditional methods for imaging orthopedic tissues. PC techniques allow both greater structural detail of features already visible in absorption images and identification of new features in tissues that produce little or no absorption contrast, such as cartilage. Cartilage is only visible in absorption images when targeted contrast agents are employed.[8] In all studies described here the features in orthopedic tissues are observed in the absence of any contrast agents.

Nearly all of the PC implementations described in the previous section have been shown to allow imaging of cartilage structure. Cartilage within knee, ankle, and shoulder joints can be observed and characterized in refraction images of both radiographs and CT.[11,39,41–44] A number of groups have used PC imaging to analyze differences in cartilage structure between healthy and arthritic joints. In absorption-based imaging, osteoarthritis is diagnosed only in the final stage of arthritis when deformation of the joint can be clearly identified due to the close proximity of bones (i.e., the diagnosis is based on the ability to image calcified tissues and not cartilage). Refraction images generated through PC imaging allow quantification of cartilage volume and identification of changes in gross cartilage structure at earlier stages, which could lead to preventive treatment and possibly a reduction in the number of joint replacement surgeries. The changes to cartilage may be identified in early stages before irreparable damage occurs.[45–47] This ability to image and quantitatively analyze cartilage structure with X-ray PC imaging suggests a significant potential for use in evaluating cartilage tissue engineering strategies.

X-ray PC imaging can also be used to image the bone–cartilage interface. Refraction images generated through a propagation-based method allow identification and differentiation of the three zones of articular cartilage (Fig. 3A).[48,49] Small-angle X-ray scatter images can also be used to identify these three zones.[48] In addition to differentiating between different cartilage regions, PC images display the interface between calcified cartilage and bone and provide detail into tendons and ligaments that are not visible in absorption images (Fig. 3B).[13,50] Lastly, refraction images can provide detail on the architecture of trabecular bone. The refraction images exploit differing refractive indices to clearly identify boundaries between solid structures and soft tissue, providing greater detail on bone structure than provided by absorption-based imaging alone. Differences in the structure and porosity of bone can be detected potentially making X-ray PC imaging a means to noninvasively monitor cortical remodeling as well as engineered bone formation.[51,52]

Vasculature

The formation of vascular networks with tissue-appropriate structure is vital to tissue engineering.[53,54] The ability to quantitatively analyze the 3D structure of vasculature in engineered tissues is essential to the evaluation of the success

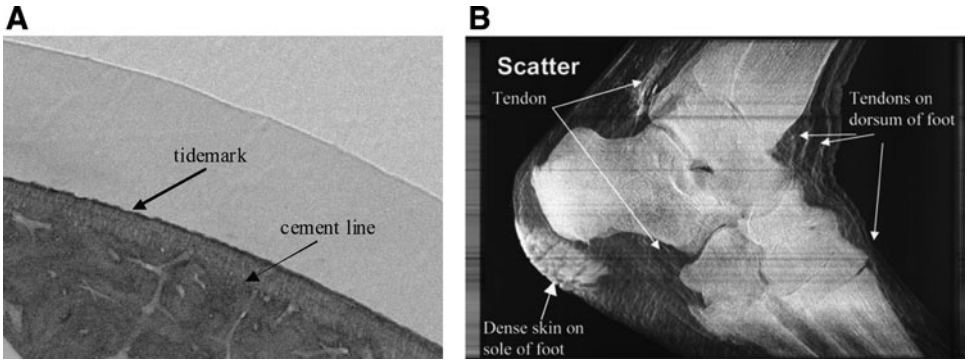

FIG. 3. Examples of X-ray PC images of orthopedic tissues. **(A)** Refraction image from propagation-based imaging of a bone–cartilage interface depicting the three zones of articular cartilage. Figure reproduced with permission from Ismail *et al.*[48] **(B)** Ultra-small-angle X-ray scatter image produced by MIR displaying tendons in a foot. Tendons are also visible in refraction images but are not shown here. Figure reproduced with permission from Wernick *et al.*[13]

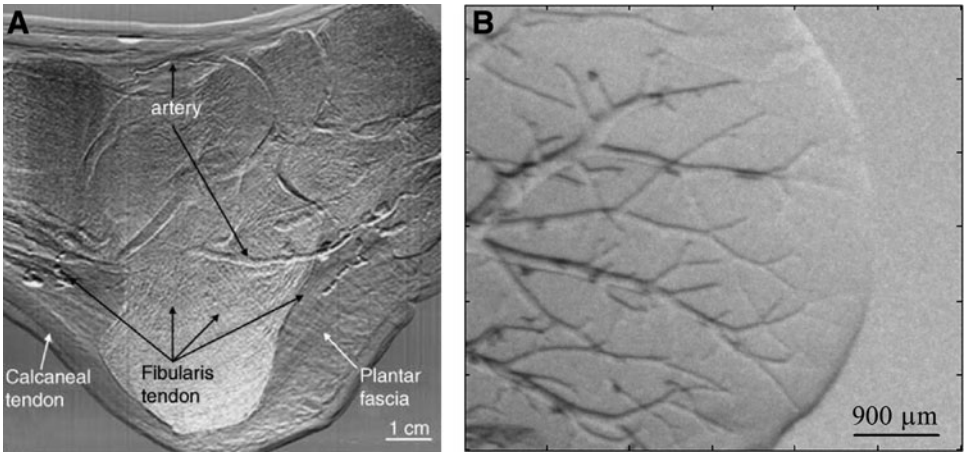

FIG. 4. Examples of X-ray PC images of vasculature produced using analyzer-based imaging **(A)** Refraction image from MIR of an ankle depicting arteries that can be seen over the bone. Figure reproduced with permission from Muehleman *et al.*[50] **(B)** Refraction image of a liver after 100 min of dehydration. Air first fills the venules generating contrast that allows imaging of the vascular tree.

of a given strategy. However, observation of blood vessels using absorption-based X-ray imaging is challenging. To image network structure, contrast agents, or corrosion casts that generate absorption contrast can be introduced and imaged using conventional X-ray techniques.[7] However, this can result in nonuniform filling of vessels and possibly the need to destroy the rest of the tissue. Complete reliance on absorption contrast leads to significant challenges when attempting to simultaneous identify multiple tissue features in a single sample (e.g., microvascular and calcified tissue structure).

Depending on vessel properties and conditions, PC techniques can provide detail on vascular structure in the absence of exogenous contrast agents. Specifically, interferometric techniques have been shown to allow insight into vascular structure within the liver resolving vessels as small as 50 μm in diameter.[55] In-line holography micrographs allowed imaging of blood vessels as small as 20 μm in diameter in the auricle region of live mice.[56,57] Arteries can be seen in MIR refraction images of human feet and thumbs even in the presence of highly absorbing and scattering calcified bone (Fig. 4A).[50]

While vessels can be detected with X-ray PC without sample manipulation, many groups exploit the large difference in refractive index between tissue and air or tissue and saline to enhance the observation of vessels. Both analyzer-based and propagation-based techniques have been implemented to image vasculature in a partially dehydrated liver (Fig. 4B).[58] This method is successful because during the drying process the veins are dehydrated first, resulting in enhanced vascular contrast before significant loss of bulk tissue volume due to overall drying. An in-line technique allowed observation of 3D microvascular networks within a porous ceramic scaffold harvested after 24 weeks of subcutaneous implantation in mice.[22] Capillaries down to 20 μm were visible in the PC images. The vascular contrast in these samples was potentially enhanced by drying the samples before imaging, but it is not clear to what level complete sample dehydration enhances vascular contrast.[59] Observation of the liver vasculature can also be enhanced by replacing blood with saline.[60] Due to the enhancement generated by air, gas-filled microbubbles currently used for ultrasonography also have the potential to generate significant vascular contrast in PC imaging.[61] While contrast agents may be required to enhance observation of vasculature, they offer a number of advantageous over microfil approaches, primarily due to the fact that tissue specific features can be separated based on distinct absorption and PC mechanisms.

Engineered tissues and biomaterials

The ability to image orthopedic tissues and blood vessels suggests that X-ray PC imaging could be used to provide important insight into the structure of engineered tissues for a number of applications. PC techniques have been investigated for imaging individual cells, biomaterials, and new tissue growing into biomaterial implants. These studies are applications of X-ray PC imaging either directly to tissue

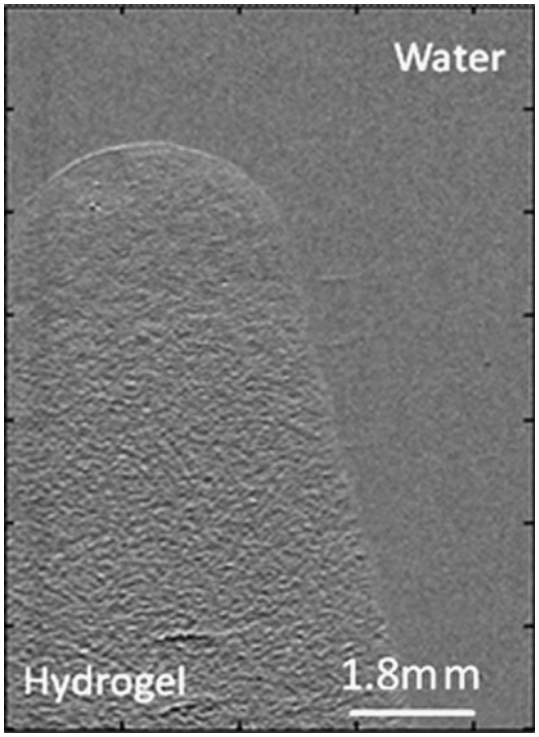

FIG. 5. X-ray refraction images allow identification of porous PEG hydrogels in water. The speckle pattern observed is due to the multiple interactions of pores and X-rays as they pass through the sample. PEG, polyethylene glycol.

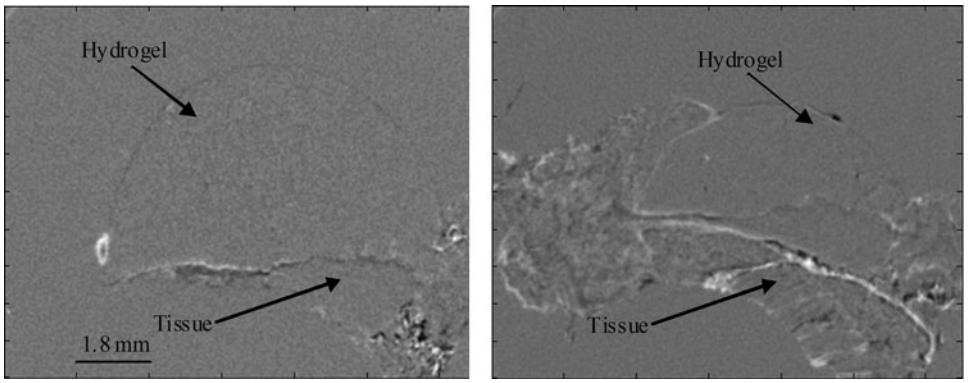

FIG. 6. Refraction CT cross sections of explanted porous PEG hydrogels. The fibrovascular tissue and hydrogel can be clearly identified.

engineering applications or to conditions similar to those encountered in tissue engineering.

Individual neurons and fibroblasts could be identified within thin collagen gels in the absence of any exogenous contrast using propagation-based PC imaging.[56,62] Propagation-based CT has also been shown to allow the identification of single chondrocytes within cartilage lacuna. The volume of a single cell could be used to estimate cell density within a region of articular cartilage from CT images.[49] Cells have also been imaged after culture on polymeric scaffolds. Edge enhancement resulting from propagation-based PC imaging allowed identification of individual fibroblasts and calvarial cells on the surface of poly(ethylene terephthalate) multifilament yarns.[63,64] A grating-based method has also been shown to successfully identify fibroblasts encapsulated within a polymeric hollow fiber containing a poly(vinyl alcohol) foam.[30] These experiments demonstrate the ability of X-ray PC to provide sufficient contrast for identification of individual cells within a biomaterial environment and that this information can be used to provide quantitative information about cell density and distribution in a given tissue or material.

Several groups have applied X-ray PC imaging toward the characterization of biomaterial scaffolds used for tissue engineering. A propagation-based imaging scheme was able to characterize the interconnected porous structure of a hydroxyapatite scaffold and to analyze the architecture of a commercial biomembrane consisting of poly (lactic acid) (PLA) and acetyl-tributylcitrate.[65,66] In these studies, the samples were imaged in air. The drying of samples is often used to enhance contrast in PC imaging due to the significant differences in X-ray refractive index between air and biomaterials/soft tissues. Recently, PC imaging has been shown to provide material details in a fully hydrated environment. Polyethylene glycol (PEG) hydrogels could be distinguished from surrounding water *in vitro* and fibrovascular tissue *ex vivo* in refraction images produced using the MIR technique.[67] PEG hydrogels consist of >90% water resulting in very low X-ray absorption. However, the MIR refraction images were sensitive to the slight difference in the refractive indices between PEG hydrogels and surrounding water, allowing the identification of hydrogel–water interfaces (Fig. 5). In addition, pores within the hydrogels resulted in image texture that was not present in nonporous gels.

Finally, X-ray PC imaging has been used as a tool to image and analyze newly formed tissue after implantation of a polymer scaffold. While most of the applications have focused on osteogenesis, a few have looked at soft tissue integration with the scaffold. Porous PEG hydrogels were implanted subcutaneously in a rat and harvested at 1 week. DEI CT allowed visualization of the integration of the hydrogel with fibrovascular tissue (Fig. 6). In-line X-ray PC CT was able to identify extracellular matrix (ECM) organization around poly(glycolic acid)–PLA copolymer fibers. The ECM was presumably deposited by cells cultured on the scaffold *in vitro*.[59] Multiple contrast mechanisms were exploited to image numerous features of the environment as the cells could be simultaneously identified after labeling with an absorption contrast agent. A combination of absorption and PC through an in-line method has also been exploited to allow observation of 3D microvascular networks within a porous ceramic scaffold.[22] The vascular networks were imaged in air without contrast agents based on PC, whereas the ceramic scaffold was visible based on absorption contrast. Bone regeneration can be observed in response to biomaterial implants using absorption-based techniques. However, refraction images can provide additional information on the quality of integration with the implant.[42,68–70] These studies provide a small glimpse of how X-ray PC techniques can be used to provide unique insight into engineered tissues grown *in vitro* and in tissue samples.

Conclusion

X-ray PC imaging offers a number of advantages over many imaging techniques currently employed in tissue engineering. The ability to obtain detailed structural information simultaneously on biomaterial, calcified tissue, and soft tissue structure with high spatial resolution and depth, often without the need for exogenous contrast, suggests its significant potential. To this point, research performed in the area of tissue engineering and biomaterials has focused on *ex vivo* sample characterization. However, future studies need to focus on the development and investigation of these techniques toward the noninvasive imaging of engineered tissues in bioreactors and *in vivo*. Further progress of the technology, especially developments that can lead to the use of available benchtop X-ray tubes, is needed to make PC imaging more easily available in the lab and clinical settings. New and existing contrast agents, such as microbubbles,[61] should also be investigated with to further improve the features that can be observed with PC techniques. Presently, very few studies exploit the multiples contrast mechanisms inherent in the PC imaging techniques (absorption,

refraction, and USAXS). Therefore, continued development and investigation of X-ray PC imaging should be a top priority for the field of tissue engineering.

Acknowledgments

Research described here has been supported in part by the Veterans Administration, the National Science Foundation (0854430, 0731201, 0546113), and the National Institute of Health (R01EB009715). The authors would like to thank Jeffery Larson for assistance with the acquisition of CT data and production of the imaging schematics.

Disclosure Statement

The authors declare that they have no competing financial interests.

References

1. Organ Procurement an Transplant Network. The U.S. Procurement and Transplantation Network and the Scientific Registry of Transplant Recipients. 2009. Available at optn.transplant.hrsa.gov/ar2009/.
2. American Society of Plastic Surgeons. 2010. Plastic and Reconstructive Surgery. Available at www.prsjounrnal.org.
3. Nam, S.Y., Mallidi, S., Zhang, G., Suggs, L., and Emelianov, S. Ultrasound and photoacoustic imaging to monitor vascular growth in tissue engineered constructs. Proc SPIE **7179,** 71790G, 2009.
4. Cancedda, R., Cedola, A., Giuliani, A., Komlev, V., Lagomarsino, S., Mastrogiacomo, M., Peyrin, F., and Rustichelli, F. Bulk and interface investigations of scaffolds and tissue-engineered bones by X-ray microtomography and X-ray microdiffraction. Biomaterials **28,** 2505, 2007.
5. Ho, S.T., and Hutmacher, D.W. A comparison of micro CT with other techniques used in the characterization of scaffolds. Biomaterials **27,** 1362, 2006.
6. Young, S., Kretlow, J.D., Nguyen, C., Bashoura, A.G., Baggett, L.S., Jansen, J.A., Wong, M., and Mikos, A.G. Microcomputed tomography characterization of neovascularization in bone tissue engineering applications. Tissue Eng Part B Rev **14,** 295, 2008.
7. Mondy, W.L., Cameron, D., Timmermans, J.P., De Clerck, N., Sasov, A., Casteleyn, C., and Piegl, L.A. Micro-CT of corrosion casts for use in the computer-aided design of microvasculature. Tissue Eng Part C Methods **15,** 729, 2009.
8. Guldberg, R., Duvall, C., Peister, A., Oest, M., Lin, A., Palmer, A., and Levenston, M. 3D imaging of tissue integration with porous biomaterials. Biomaterials **29,** 3757, 2008.
9. Faraj, K.A., Cuijpers, V., Wismans, R.G., Walboomers, F., Jansen, J.A., Van Kuppevelt, T., and Daamen, W.F. Microcomputed tomographical imaging of soft biological materials using contrast techniques. Tissue Eng Part C Methods **15,** 493, 2009.
10. Mizutani, R., Takeuchi, A., Uesugi, K., Takekoshi, S., Osamura, R.Y., and Suzuki, Y. X-ray microtomographic imaging of three-dimensional structure of soft tissues. Tissue Eng Part C Methods **14,** 359, 2008.
11. Lewis, R.A. Medical phase contrast x-ray imaging: current status and future prospects. Phys Med Biol **49,** 3573, 2004.
12. Mayo, S., Davis, T., Gureyev, T., Miller, P., Paganin, D., Pogany, A., Stevenson, A., and Wilkins, S. X-ray phase-contrast microscopy and microtomography. Opt Express **11,** 2289, 2003.
13. Wernick, M.N., Wirjadi, O., Chapman, D., Zhong, Z., Galatsanos, N.P., Yang, Y., Brankov, J.G., Oltulu, O., Anastasio, M.A., and Muehleman, C. Multiple-image radiography. Phys Med Biol **48,** 3875, 2003.
14. Wu, X., and Liu, H. Clinical implementation of x-ray phase-contrast imaging: theoretical foundations and design considerations. Med Phys **30,** 2169, 2003.
15. Arfelli, F., Assante, M., Bonvicini, V., Bravin, A., Cantatore, G., Castelli, E., Dalla Palma, L., Di Michiel, M., Longo, R., Olivo, A., Pani, S., Pontoni, D., Poropat, P., Prest, M., Rashevsky, A., Tromba, G., Vacchi, A., Vallazza, E., and Zanconati, F. Low-dose phase contrast x-ray medical imaging. Phys Med Biol **43,** 2845, 1998.
16. Anastasio, M.A., Chou, C.-Y., Zysk, A.M., and Brankov, J. Analysis of ideal observer signal detectability in phase-contrast imaging employing linear shift-invariant optical systems. J Opt Soc Am A **27,** 2648, 2010.
17. Paganin, D.M. Coherent X-Ray Optics. Oxford, England: Oxford University Press, 2006.
18. Bech, M., Jensen, T.H., Bunk, O., Donath, T., David, C., Weitkamp, T., Le Duc, G., Bravin, A., Cloetens, P., and Pfeiffer, F. Advanced contrast modalities for X-ray radiology: phase-contrast and dark-field imaging using a grating interferometer. Z Med Phys **20,** 7, 2010.
19. Zhou, S., and Brahme, A. Development of phase-contrast X-ray imaging techniques and potential medical applications. Phys Med **24,** 129, 2008.
20. Kitchen, M.J., Paganin, D.M., Uesugi, K., Allison, B.J., Lewis, R.A., Hooper, S.B., and Pavlov, K.M. Phase contrast image segmentation using a Laue analyser crystal. Phys Med Biol **56,** 515, 2011.
21. Yan, A., Wu, X., and Liu, H. An attenuation-partition based iterative phase retrieval algorithm for in-line phase-contrast imaging. Opt Express **16,** 13330, 2008.
22. Komlev, V.S., Mastrogiacomo, M., Peyrin, F., Cancedda, R., and Rustichelli, F. X-ray synchrotron radiation pseudo-holotomography as a new imaging technique to investigate angio- and microvasculogenesis with no usage of contrast agents. Tissue Eng Part C Methods **15,** 425, 2009.
23. Zehbe, R., Haibel, A., Riesemeier, H., Gross, U., Kirkpatrick, C.J., Schubert, H., and Brochhausen, C. Going beyond histology. Synchrotron micro-computed tomography as a methodology for biological tissue characterization: from tissue morphology to individual cells. J R Soc Interface **7,** 49, 2009.
24. Momose, A. Phase-sensitive imaging and phase tomography using X-ray interferometers. Opt Express **11,** 2303, 2003.
25. Yoneyama, A., Momose, A., Koyama, I., Seya, E., Takeda, T., Itai, Y., Hirano, K., and Hyodo, K. Large-area phase-contrast X-ray imaging using a two-crystal X-ray interferometer. J Synchrotron Radiat **9,** 277, 2002.
26. Wang, Z., Zhu, P., Huang, W., Yuan, Q., Liu, X., Zhang, K., Hong, Y., Zhang, H., Ge, X., Gao, K., and Wu, Z. Quantitative coherence analysis with an X-ray Talbot–Lau interferometer. Anal Bioanal Chem **397,** 2091, 2010.
27. Chen, G.H., Bevins, N., Zambelli, J., and Qi, Z. Small-angle scattering computed tomography (SAS-CT) using a Talbot-Lau interferometerand a rotating anode x-ray tube: theory and experiments. Opt Express **18,** 12960, 2010.
28. Pfeiffer, F., Weitkamp, T., Bunk, O., and David, C. Phase retrieval and differential phase-contrast imaging with low-brilliance X-ray sources. Nat Phys **2,** 258, 2006.
29. Jiang, M., Wyatt, C.L., and Wang, G. X-ray phase-contrast imaging with three 2D gratings. Int J Biomed Imaging **2008,** 827152, 2008.

30. Mcdonald, S.A., Marone, F., Hintermüller, C., Bensadoun, J.C., Aebischer, P., and Stampanoni, M. High-throughput, high-resolution X-ray phase contrast tomographic microscopy for visualisation of soft tissue. J Phys Conf Ser **186,** 012043, 2009.
31. Zhu, P., Zhang, K., Wang, Z., Liu, Y., Liu, X., Wu, Z., Mcdonald, S.A., Marone, F., and Stampanoni, M. Low-dose, simple, and fast grating-based X-ray phase-contrast imaging. Proc Natl Acad Sci USA **107,** 13576, 2010.
32. Chapman, D., Thomlinson, W., Johnston, R.E., Washburn, D., Pisano, E., Gmur, N., Zhong, Z., Menk, R., Arfelli, F., and Sayers, D. Diffraction enhanced x-ray imaging. Phys Med Biol **42,** 2015, 1997.
33. Dilmanian, F.A., Zhong, Z., Ren, B., Wu, X.Y., Chapman, L.D., Orion, I., and Thomlinson, W.C. Computed tomography of x-ray index of refraction using the diffraction enhanced imaging method. Phys Med Biol **45,** 933, 2000.
34. Chou, C.-Y., Anastasio, M.A., Brankov, J.G., Wernick, M.N., Brey, E.M., Connor, D.M., and Zhong, Z. An extended diffraction-enhanced imaging method for implementing multiple-image radiography. Phys Med Biol **52,** 1923, 2007.
35. Rigon, L., Besch, H., Arfelli, F., Menk, R., Heitner, G., and Plothow-Besch, H. A new DEI algorithm capable of investigating sub-pixel structures. J Phys D Appl Phys **36,** A107, 2003.
36. Rigon, L., Arfelli, F., and Menk, R.-H. Three-image diffraction enhanced imaging algorithm to extract absorption, refraction, and ultrasmall-angle scattering. Appl Phys Lett **90,** 114102, 2007.
37. Khelashvili, G., Brankov, J.G., Chapman, D., Anastasio, M.A., Yang, Y., Zhong, Z., and Wernick, M.N. A physical model of multiple-image radiography. Phys Med Biol **51,** 221, 2006.
38. Ando, M., Maksimenko, A., Sugiyama, H., Pattanasiriwisawa, W., Hyodo, K., and Uyama, C. Simple X-ray dark- and bright-field imaging using achromatic laue optics. Jpn J Appl Phys **41,** L1016, 2002.
39. Kunisada, T., Shimao, D., Sugiyama, H., Takeda, K., Ozaki, T., and Ando, M. X-ray dark field imaging of human articular cartilage: possible clinical application to orthopedic surgery. Eur J Radiol **68,** S18, 2008.
40. Shimao, D., Kunisada, T., Sugiyama, H., and Ando, M. Shift-and-add tomosynthesis of a finger joint by X-ray dark-field imaging: difference due to tomographic angle. Eur J Radiol **68,** S27, 2008.
41. Brankov, J.G., Wernick, M.N., Yang, Y., Li, J., Muehleman, C., Zhong, Z., and Anastasio, M.A. A computed tomography implementation of multiple-image radiography. Med Phys **33,** 278, 2006.
42. Coan, P., Mollenhauer, J., Wagner, A., Muehleman, C., and Bravin, A. Analyzer-based imaging technique in tomography of cartilage and metal implants: a study at the ESRF. Eur J Radiol **68,** 16074, 2008.
43. Li, J., Zhong, Z., Connor, D., Mollenhauer, J., and Muehleman, C. Phase-sensitive X-ray imaging of synovial joints. Osteoarthritis Cartilage **17,** 1193, 2009.
44. Muehleman, C., Li, J., Wernick, M., Brankov, J., Kuettner, K., and Zhong, Z. Yes, you can see cartilage with X-rays; diffraction enhanced X-ray imaging for soft and hard tissues. J Musculoskelet Neuronal Interact **4,** 369, 2004.
45. Crittell, S., Cheung, K., Hall, C., Ibison, M., Nolan, P., Page, R., Scraggs, D., and Wilkinson, S. Diffraction enhanced imaging of normal and arthritic mice feet. Nucl Instrum Methods Phys Res A **573,** 126, 2007.
46. Muehleman, C., Fogarty, D., Reinhart, B., Tzvetkov, T., Li, J., and Nesch, I. In-laboratory diffraction-enhanced X-ray imaging for articular cartilage. Clin Anat **23,** 530, 2010.
47. Wagner, A., Aurich, M., Sieber, N., Stoessel, M., Wetzel, W., Schmuck, K., Lohmann, M., Reime, B., Metge, J., and Coan, P. Options and limitations of joint cartilage imaging: DEI in comparison to MRI and sonography. Nucl Instrum Methods Phys Res A **548,** 47, 2005.
48. Ismail, E.C., Kaabar, W., Garrity, D., Gundogdu, O., Bunk, O., Pfeiffer, F., Farquharson, M.J., and Bradley, D.A. X-ray phase contrast imaging of the bone–cartilage interface. Appl Radiat Isot **68,** 767, 2010.
49. Zehbe, R., Goebbels, J., Ibold, Y., Gross, U., and Schubert, H. Three-dimensional visualization of *in vitro* cultivated chondrocytes inside porous gelatine scaffolds: a tomographic approach. Acta Biomater **6,** 2097, 2010.
50. Muehleman, C., Li, J., Zhong, Z., Brankov, J.G., and Wernick, M.N. Multiple-image radiography for human soft tissue. J Anat **208,** 115, 2006.
51. Cooper, D.M.L., Bewer, B., Wiebe, S., Wysokinski, T.W., and Chapman, D. Diffraction enhanced X-ray imaging of the distal radius: a novel approach for visualization of trabecular bone architecture. Can Assoc Radiol J 2010 [Epub ahead of print]; DOI: 10.1016/j.carj.2010.04.015
52. Menk, R., Rigon, L., and Arfelli, F. Diffraction-enhanced X-ray medical imaging at the ELETTRA synchrotron light source. Nucl Instrum Methods Phys Res A **548,** 213, 2005.
53. Francis, M.E., Uriel, S., and Brey, E.M. Endothelial cell-matrix interactions in neovascularization. Tissue Eng Part B Rev **14,** 19, 2008.
54. Francis-Sedlak, M.E., Moya, M.L., Huang, J., Lucas, S.A., Chandrasekharan, N., Larson, J.C., Cheng, M.H., and Brey, E.M. Collagen glycation alters neovascularization *in vitro* and *in vivo*. Microvasc Res **80,** 3, 2010.
55. Momose, A., Takeda, T., and Itai, Y. Blood vessels: depiction at phase-contrast X-ray imaging without contrast agents in the mouse and rat-feasibility study. Radiology **217,** 593, 2000.
56. Hwu, Y., Je, J., and Margaritondo, G. Real-time radiology in the microscale. Nucl Instrum Methods Phys Res A **551,** 108, 2005.
57. Hwu, Y., Tsai, W.L., Je, J.H., Seol, S.K., Kim, B., Groso, A., Margaritondo, G., Lee, K.-H., and Seong, J.-K. Synchrotron microangiography with no contrast agent. Phys Med Biol **49,** 501, 2004.
58. Laperle, C.M., Hamilton, T.J., Wintermeyer, P., Walker, E.J., Shi, D., Anastasio, M.A., Derdak, Z., Wands, J.R., Diebold, G., and Rose-Petruck, C. Low density contrast agents for x-ray phase contrast imaging: the use of ambient air for x-ray angiography of excised murine liver tissue. Phys Med Biol **53,** 6911, 2008.
59. Albertini, G., Giuliani, A., Komlev, V., Moroncini, F., Pugnaloni, A., Pennesi, G., Belicchi, M., Rubini, C., Rustichelli, F., Tasso, R., and Torrente, Y. Organization of extracellular matrix fibers within polyglycolic acid-polylactic acid scaffolds analyzed using X-ray synchrotron-radiation phase-contrast micro computed tomography. Tissue Eng Part C Methods **15,** 403, 2009.
60. Takeda, T. Vessel imaging by interferometric phase-contrast X-ray technique. Circulation **105,** 1708, 2002.
61. Arfelli, F., Rigon, L., and Menk, R.H. Microbubbles as x-ray scattering contrast agents using analyzer-based imaging. Phys Med Biol **55,** 1643, 2010.
62. Hwu, Y., Tsai, W.L., Chang, H.M., Yeh, H.I., Hsu, P.C., Yang, Y.C., Su, Y.T., Tsai, H.L., Chow, G.M., and Ho, P.C.

Imaging cells and tissues with refractive index radiology. Biophys J **87,** 4180, 2004.
63. Thurner, P., Muller, B., Beckmann, F., Weitkamp, T., Rau, C., Muller, R., Hubbell, J.A., and Sennhauser, U. Tomography studies of human forskin fibroblasts on polymer yarns. Nucl Instrum Methods Phys Res B **200,** 397, 2003.
64. Thurner, P., Müller, R., Raeber, G., Sennhauser, U., and Hubbell, J.A. 3D morphology of cell cultures: a quantitative approach using micrometer synchrotron light tomography. Microsc Res Tech **66,** 289, 2005.
65. Baruchel, J., Lodini, A., Romanzetti, S., Rustichelli, F., and Scrivani, A. Phase-contrast imaging of thin biomaterials. Biomaterials **22,** 1515, 2001.
66. Rustichelli, F., Romanzetti, S., Dubini, B., Girardin, E., Raven, C., Snigirev, A., and Rizzi, G. Phase-contrast microtomography of thin biomaterials. J Mater Sci Mater Med **15,** 1053, 2004.
67. Brey, E.M., Appel, A., Chiu, Y.C., Zhong, Z., Cheng, M.H., Engel, H., and Anastasio, M.A. X-ray imaging of poly(ethylene glycol) hydrogels without contrast agents. Tissue Eng Part C Methods **16,** 1597, 2010.
68. Wagner, A., Sachse, A., Keller, M., Aurich, M., Wetzel, W.D., Hortschansky, P., Schmuck, K., Lohmann, M., Reime, B., Metge, J., Arfelli, F., Menk, R., Rigon, L., Muehleman, C., Bravin, A., Coan, P., and Mollenhauer, J. Qualitative evaluation of titanium implant integration into bone by diffraction enhanced imaging. Phys Med Biol **51,** 1313, 2006.
69. Weiss, P. Synchrotron X-ray microtomography (on a micron scale) provides three-dimensional imaging representation of bone ingrowth in calcium phosphate biomaterials. Biomaterials **24,** 4591, 2003.
70. Yeom, J., Chang, S., Park, J.K., Je, J.H., Yang, D.J., Choi, S.K., Shin, H.I., Lee, S.J., Shim, J.H., Cho, D.W., and Hahn, S.K. Synchrotron X-ray bio-imaging of bone regeneration by artificial bone substitute of MGSB and hyaluronate hydrogels. Tissue Eng Part C Methods **16,** 1059, 2010.

Address correspondence to:
Eric M. Brey, Ph.D.
Department of Biomedical Engineering and Pritzker Institute of Biomedical Science and Engineering
Illinois Institute of Technology
3255 South Dearborn St.
Chicago, IL 60616

E-mail: brey@iit.edu

Received: April 21, 2011
Accepted: June 15, 2011
Online Publication Date: July 29, 2011